

Plasma Stainless Steel Wall Interaction of the LHD

SUZUKI Hajime*, OHYABU Nobuyoshi, KOMORI Akio, MOTOJIMA Osamu
and LHD experimental group 1,2
National Institute for Fusion Science, Toki-shi 509-52, Japan

(Received: 18 January 2000 / Accepted: 8 June 2000)

Abstract

For steady state plasma operation, the study of plasma wall interaction is very important. The Large Helical Device (LHD) has a plasma vacuum vessel, which is made of stainless steel. The particle balance of plasma experiments was studied by a fast ionization gauge (FIG), which is operational in a high magnetic field. Plasma discharge experiments of the LHD have been carried out using hydrogen and helium gas. In the case of helium plasma discharge experiments, no or very few missing particles could be detected. However, in the case of hydrogen plasma discharge experiments, almost half of the input particles have disappeared. After a hydrogen plasma discharge, gas desorption from the wall has been measured. The gas desorption has two kinds of time constants. Although the particles from the gas desorption have been added to the balance, still missing particles exist. These stay in the wall for a long time. This result indicates that two kinds of trapped state of hydrogen particles exist in stainless steel. Two kinds of diffusion constants for steel below 500 K have been reported. The pressure curves of the LHD experiments consists with this report.

Keywords:

hydrogen, helium, stainless steel, plasma-wall interaction, wall pumping effect, diffusion, lattice defect, hydrogen embrittlement.

1. Introduction

Stainless steel is often used for ultra high vacuum vessels. However, it is known that steel contains hydrogen particle in the bulk. Thus, if a stainless steel vacuum vessel would be used for a plasma vacuum vessel, characteristics of hydrogen stainless steel interaction must be studied. From a point of view of plasma control, absorption and desorption of hydrogen particles from a stainless steel wall are important. And from a point of view of material, a mechanism of trapping of hydrogen and hydrogen embrittlement are important. Especially, they are important for steady state operation under high energy and high particle flux condition.

There have been several studies on hydrogen in

steel. However, the hydrogen particles of the studies are naturally-exist hydrogen in the steel or introduced by chemical method, electric method and abrasion method. It must be studied whether hydrogen particles in steel, which is implanted by plasma, have same feature or not.

The LHD plasma experiment has been carried out in a stainless steel vacuum vessel using hydrogen or helium working gas [1]. Wall-pumping effect has been studied by investigating the defects in the particle balance. The characteristics of trap site of hydrogen in the steel has been studied by analyzing the pressure curve of desorption. This study shows where and how the hydrogen particles are trapped in the stainless steel wall of the LHD.

*Corresponding author's e-mail: hsuzuki@LHD.nifs.ac.jp

2. Apparatus

The plasma vacuum vessel of the LHD is made of stainless steel SUS316L (Fe:70%, Cr:17%, Ni:11%, Mo:2%), with a thickness of 15 mm. The volume contained in the vacuum vessel is 210 m³, and the total area including ports is about 730 m². Carbon armor tiles for the neutral beam injectors (NBI) with a surface area of about 3 m² were installed. It was only carbon area in the vacuum vessel during the second campaign of the LHD experiment. The temperature of the vacuum vessel is kept to about 300 K by cooling water. The plasma volume is about 30 m³. The ratio between the plasma volume and the vacuum vessel volume is large compared with other plasma devices.

The vacuum vessel is pumped out by two cryo pumps and four turbo molecular pumps. The total and partial pressures are monitored by pressure gauges and a quadruple mass spectrometer. One of the pressure gauges is fast ionization gauge (FIG), which is installed at 7.5 U port, about 3 m far from plasma surface. Since the FIG is operational in a high magnetic field [2], the pressure in the vacuum vessel can be measured. CAMAC system starts recording the pressure data of the FIG after trigger signal with a sampling speed of 100 μ s, and it stops recording after the plasma discharge is finished. The ordinary measuring time is 13 sec. So the neutral gas pressure before, during, and after a plasma discharge is measured with a very high frequency. Using the pressure decay curve, the effective pumping speed can be determined. The effective pumping speed of hydrogen gas is 67 m³/s and the effective pumping speed of helium gas is 17 m³/s.

The hydrogen and the helium gas are introduced through piezo valves. The voltage of the piezo valve is also recorded, and total amount of inlet gas is calculated using these data. Therefore the particle balance can be determined.

The plasma vacuum vessel is un-bakable, because of a protection for the super conducting magnets. A surface conditioning has been carried out by helium glow discharge or ECR-DC before the plasma experiments at night.

3. Experimental

The experiments have been carried out using hydrogen and helium gas. Fig. 1(a) shows a typical pressure curve of the hydrogen plasma experiment. When ECH heating starts, the pressure decreases by ionization. The pressure increases a little by NBI heating. This is the well known effect that heating

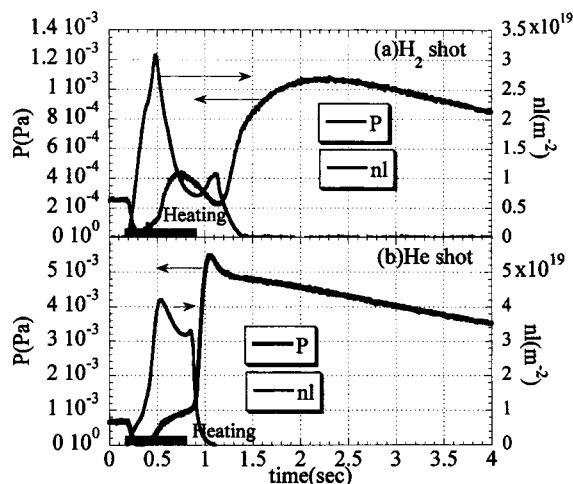


Fig. 1 Typical pressure curves of hydrogen shot(a) and helium shot(b) with line density curves.

power decreases the particle confinement time. After stopping the heating, the plasma disappears, and the pressure increases by recombination of ions. However the pressure still increases after the plasma has completely disappeared. This is explained by an outgassing from the wall. Then the pressure decays by pumping of the cryo pumps and the turbo molecular pumps. Fig. 1(b) shows a typical pressure curve of the helium plasma experiment. In the case of helium, the pressure curve is almost the same as in the hydrogen case before the heating stops. However the pressure curve of the helium gas case is different from the hydrogen gas case after the heating stopped. The pressure rises by recombination then drops a little. This drop may be explained by absorption on a clean surface, which has been produced by helium bombardment during the plasma discharge.

The most significant difference between the hydrogen and helium discharge is difference in the gas balance, which is the result of the wall-pumping. Fig. 2(a) shows pressure curves for the same hydrogen gas puffing condition with/without plasma. Fig. 2(b) displays pressure curves in the same helium gas puffing condition with/without plasma. In the helium case, no or very small missing particles exist. However in the case of hydrogen, almost half of the input hydrogen particle have disappeared. Fig. 3 is a plot of the total amount of missing particles after plasma shots as a function of the maximum stored energy. There is an energy threshold of wall pumping at 80 kJ. When the stored energy exceeds 80 kJ, hydrogen particles have always been absorbed in

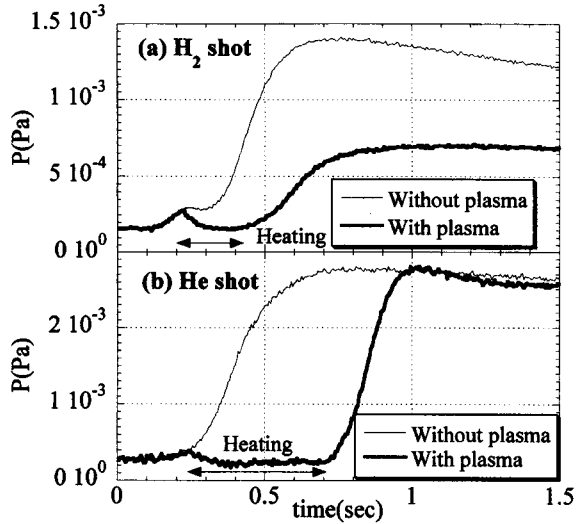


Fig. 2 Pressure curves of hydrogen(a) and helium(b) experiment with/without plasma heating under same gas puff conditions.

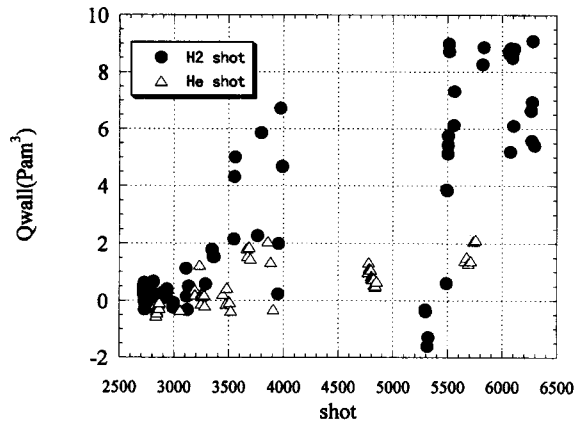


Fig. 3 Total amounts of missing particles after hydrogen and helium shots as a function of maximum stored energy of the shots.

the wall. No saturation of the wall has been observed during the second campaign of the LHD experiment. The total amount of the implanted hydrogen particles have not reach the saturation level during the experimental time of one day. The saturation level is discussed in the next section. The wall conditionings at night have been effective for removing the hydrogen particles in the wall, and the wall has been recovered.

4. Discussion

Without plasma, wall pumping has not been observed. The wall pumping is obviously caused by

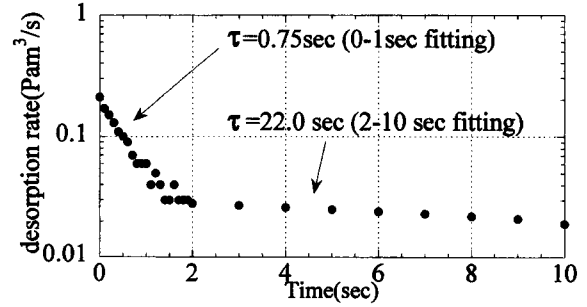


Fig. 4 Desorption rate of hydrogen gas from the wall of the LHD. $T = 0$ sec is a same time as $T = 1.5$ sec of Fig. 1(a).

implantation, and not by surface absorption. High energetic hydrogen atoms, which are produced by charge exchange interaction, have been implanted into the wall. The time constant of desorption is about a few seconds. If a source of outgassing is the surface, the time constant should be about 10^{-12} sec [3]. This points out that the source of outgassing is not the surface.

R. Calder and G. Lewin have pointed out that the desorption rate of hydrogen gas from a stainless steel could be explained by a diffusion to the surface from the interior of the metal [4]. They have been calculated the desorption rate as,

$$\begin{aligned} \dot{Q} &= D \left(\frac{\partial c}{\partial X} \right)_{X=0} \\ &= \frac{4c_0 D}{d} \sum_{n=0}^{\infty} \exp \left\{ - \left(\frac{\pi(2n+1)}{d} \right)^2 Dt \right\} \end{aligned}$$

where c is the concentration of hydrogen and d is the depth where hydrogen particles exist. For $Dt/d^2 > 0.025$, which is the case in many practical situation, the desorption rate is written by,

$$\dot{Q} = \frac{4c_0 D}{d} \exp \left\{ - \frac{\pi^2}{d^2} Dt \right\}$$

and the time constant is given by $\tau = d^2/\pi^2 D$.

In the LHD case, the desorption rate is shown in Fig. 4, which is calculated using the same data of Fig. 1(a) after 1.5 sec. It looks as if two kinds of constant exist with values of 0.75 sec and 22.0 sec, i.e. there are two kinds of trapped states of hydrogen in stainless steel.

R.C. Frank *et al.* have reported two different diffusion coefficients of hydrogen in steel (C:0.09%, Cr:0.01%, Mn:0.35%, Ni:0.05%, Mn:1.02%) in a temperature range of 25°C–90°C for the same sample [5]. The first coefficient has been measured by a build

up method and is

$$D = 5.0 \times 10^{-3} \exp \left[-\frac{3400 \text{ cal/mol}}{RT} \right] \text{ cm}^2 / \text{ sec} .$$

and the second coefficient by a decay method and is

$$D = 1.90 \times 10^{-2} \exp \left[-\frac{6320 \text{ cal/mol}}{RT} \right] \text{ cm}^2 / \text{ sec} .$$

R.C. Frank *et al.* have pointed out that the two sets of diffusion coefficients could not be attributed to an abrasive process. They have also pointed out that the two sets of diffusion coefficients have a temporal dependence. In general, the measured diffusion coefficients below 500 K vary [5-7].

Thermal desorption spectroscopy (TDS) analysis of hydrogen in steel shows a double peak structure [8,9]. The sample of Ref. 8 is SUS316L, and the sample of Ref. 9 is pearlite structure steel. M. Nagumo has reports in Ref. 9 that the first peak decreases dramatically after 48 hour from stopping of solution of hydrogen, keeping the sample at room temperature. This result also shows a time effect of two kinds of trapped state. Since stainless steel is alloy, SUS316L is not completely same as Frank's steel. And SUS316L is austenitic steel in contrast with Nagumo's pearlite structure steel. In spite of these differences, characteristics of hydrogen particles in steel reported by these references coincide with a characteristic of hydrogen in the LHD case.

A variety of measured diffusion coefficients and solution ratios of hydrogen in steel below 500 K have been reported [9]. These varieties and two kinds of trapped state are explained by several kinds of trapping sites. The tight trapping site with high activation energy is considered to be from lattice defects [9,10]. At first, implanted hydrogen particles are trapped at loose trapping sites, then diffuse with low activation energy. Some part of the hydrogen particles reach the surface and are released. The other parts of the hydrogen particles reach the tight trapping site and stay there. This is a scenario of hydrogen desorption from the stainless steel wall of the LHD

If the hydrogen has been trapped at lattice defects, the total amount of pumped particle and desorption curve should be changed historically. However, no significant change has been observed during the second campaign of the LHD experiments. This study should be continued for a longer term.

The loose-trapped hydrogen particles are important from a point of view of recycling control. Tight-trapped hydrogen particles are important from a point of view of

hydrogen saturation level and hydrogen embrittlement. These are especially important under high energy, high particle flux steady state operation. Nagumo has pointed out that an annealing over 500 K is effective for recovering lattice defects [9].

5. Conclusion

Features of the wall pumping effect of the stainless wall of the LHD have been studied using FIG data. The wall pumping effects have been observed after hydrogen plasma shots with a maximum stored energy over 80 kJ. In the case of helium shots, no or few wall pumping effects have been observed.

Two kinds of hydrogen trap sites in stainless steel have been found by analyzing the desorption curves after the hydrogen plasma shot. This result consists with the old TDS experiments or measurements of diffusion coefficient of steel.

The implanted hydrogen particles diffuse in the steel with a low activation energy. Then they trapped at a site with a high activation energy

Acknowledgements

The author is grateful to the people in the experimental group and operators of the LHD, especially, to Dr. A. Sagara, Dr. Y. Hirooka, Dr. R. Sakamoto, Dr. J. Miyazawa and Dr. S. Masuzaki for useful discussions and help.

Appendix

A diffusion coefficient of SUS316L over 500 K has been reported by Y. Ishikawa *et al.* [11]. If the diffusion coefficient of 300 K would be estimated by extrapolating the data of Ref.11, the diffusion constant of 300 K is $D = 10^{-11} \text{ cm}^2/\text{sec}$. It is much smaller than Franc's steel. In general, Ti, Zr, Cr, Mn, Si and C make diffusion coefficient smaller. If Cr reaches to 12%, the activation energy becomes two times higher [12]. This may be a reason why the diffusion coefficient of SUS316L is small.

References:

- [1] O. Motojima *et al.*, Phys. Plasma **6**, 1843 (1999).
- [2] C.C. Klepper, *et al.*, J. Vac. Sci. and Technol. **A11**, 446 (1993).
- [3] J. Frankel, Z. Physik., **26**, 117 (1923).
- [4] R. Calder and G. Lewin, Brit. J. Appl. Phys. **18**, 1459 (1967).
- [5] R.C. Frank, D.E. Swets and D.L. Fry, J. Appl. Phys. **29**, 892 (1958).

- [6] W.Y. Choo and J.Y. Lee, *Metall. Trans. A*, **13A**, 135 (1982).
- [7] K. Kiuchi and R.B. McLellan, *Acta Metall.*, **31**, 961 (1983).
- [8] Y. Ishikawa, Y. Koguchi and K. Odaka, *J. Vac Sci. Technol.* **A9**, 250 (1991).
- [9] M. Nagumo, *J. Vac. Soc. Jpn.* **42**, 1042 (1999), in Japanese.
- [10] R.A. Oriani, *Acta Metall.*, **18**, 147 (1970).
- [11] Y. Ishikawa, T. Yoshimura and M. Arai, *Vacuum* **47**, 357 (1996).
- [12] P.V. Gelid and R.A. Ryabov, *ΦMM, γ5*, **B1**, 191 (1957), in Russia.